Genome-wide association studies in Japanese women identified genetic loci associated with wrinkles and sagging

Ryosuke Okuno[1, 2], Yu Inoue[1, 2], Yuichi Hasebe[1, 2], Toshio Igarashi[1], Mika Kawagishi-Hotta[1, 2], Takaaki Yamada[1], Seiji Hasegawa[1, 2]

[1] *Research Laboratories, Nippon Menard Cosmetic Co., Ltd., Nagoya, Aichi, Japan.*
[2] *Nagoya University-MENARD Collaborative Research Chair, Nagoya University Graduate School of Medicine, Nagoya, Aichi, Japan.*

To whom correspondence should be addressed: Ryosuke Okuno, Research Laboratories, Nippon Menard Cosmetic Co., Ltd., 2-7, Torimi-cho, Nishiku, Nagoya, Aichi, Japan. Tel.: +81-52-531-6263; Fax: +81-52-531-6277; E-mail: okuno.ryousuke@menard.co.jp

word count: 4054
(excluding abstract, title page, keywords, tables and references/bibliography)

Number of display items: 3 Figures, 5 supplementary figures, 2 tables, 7 supplementary tables.

Abstract

Wrinkles and sagging are caused by various factors, such as ultraviolet rays; however, recent findings demonstrated that some individuals are genetically predisposed to these phenotypes of skin aging. The contribution of single nucleotide polymorphisms (SNPs) to the development of wrinkles and sagging has been demonstrated in genome-wide association studies (GWAS). However, these findings were mainly obtained from European and Chinese populations. Limited information is currently available on the involvement of SNPs in the development of wrinkles and sagging in a Japanese population. Therefore, we herein performed GWAS on wrinkles at the outer corners of the eyes and nasolabial folds in 1041 Japanese women. The results obtained revealed that 5 SNPs (19p13.2: rs2303098 ($p = 3.39\times10^{-8}$), rs56391955 ($p = 3.39\times10^{-8}$), rs67560822 ($p = 3.50\times10^{-8}$), rs889126 ($p = 3.78\times10^{-8}$), rs57490083 ($p = 3.99\times10^{-8}$)) located within the *COL5A3* gene associated with wrinkles at the outer corners of the eyes. Regarding nasolabial folds, 8q24.11 (rs4876369; $p = 1.05\times10^{-7}$, rs6980503; $p = 1.25\times10^{-7}$, rs61027543; $p = 1.25\times10^{-7}$, rs16889363; $p = 1.38\times10^{-7}$) was suggested to be associated with *RAD21* gene expression. These SNPs have not been reported in other populations, and were first found in Japanese women population. These SNPs may be used as markers to examine the genetic predisposition of individuals to wrinkles and sagging.

Key words

genome-wide association studies

single nucleotide polymorphism

wrinkles

sagging

Japanese females

Introduction

In the field of beauty, wrinkles and sagging are the most prominent phenotypes of aging phenomena on the face, and effective methods for their prevention and improvement are desired. Wrinkles and sagging are primarily caused by external factors, such as ultraviolet rays, as well as the age-related disintegration of collagen fibers[1,2], decreased collagen production by dermal fibroblasts[3,4], and the increased production of matrix metalloproteinases[5–7]. Genome-wide association studies (GWAS) on skin aging have recently been conducted, and the findings obtained clearly showed that some individuals were genetically predisposed to more rapid skin aging. Single nucleotide polymorphisms (SNPs) have been associated with a number of skin properties, including wrinkles, eyelid sagging, skin color, the type of sunburn, and skin barrier function[8–14]. The relationships between these phenotypes and SNPs markedly differ depending on race, and, thus, in order to identify SNPs that are associated with the phenotypes of a specific racial group, analyses of this racial population are needed[10]. GWAS have been performed on European and Chinese populations, and identified rs10476781 (*NMUR2*), rs28392847 (*SHC4*), and rs76053540 (*MYH11*) as SNPs associated with wrinkles and sagging[9,10]. However, few GWAS have been conducted on skin types in Japanese populations. We previously conducted GWAS on the constitution and quality of skin in a Japanese female population and identified SNPs associated with nine phenotypes, including the sunburn type, skin spots, facial flushing, and the frequency of rough skin[15]. With the aim of clarifying the genetic predisposition of a Japanese population to wrinkles and sagging and thereby providing effective methods for their prevention and improvement, we herein report the results of GWAS on the involvement of genotypes in the development of these phenotypes of skin aging in a

Japanese population.

Materials and methods

Study population

A total of 1,200 healthy Japanese women with a mean age of 49.1 years were enrolled in the present study. Following a detailed explanation of the purpose and contents of the study with documentation, all subjects provided their written informed consent to participate. The Ethics Review Board of our company approved the protocol of the present study.

Previous studies demonstrated that wrinkles in exposed areas increase with age. Since structural changes in tissues, such as the fragmentation and disorganization of collagen fibers, were found to be significant, particularly in individuals older than 60 years[16], women younger and older than 60 years old were selected as subgroups.

Genotyping and quality control

Each subject provided a saliva sample using a saliva sampling kit (Genesis Healthcare, Tokyo, Japan). A Maxwell RSC Stabilized Saliva DNA Kit (Promega, Madison, WI, USA) was employed to extract genomic DNA from saliva, which was then subjected to genotyping using an Asian Screening Array (Illumina, San Diego, CA, USA). Approximately 650,000 SNPs were identified. Subjects and SNPs with a call rate of <0.98 in a genetic statistical analysis using PLINK software[17] (www.cog-genomics.org/plink/1.9/) and SNPs with a p-value $<1\times10^{-3}$ in the Hardy-Weinberg equilibrium probability test or a minor allele frequency (MAF) <5% were excluded from subsequent analyses. Identity-by-descent (IBD) similarity was determined using PLINK software to eliminate unidentified kinship from the genotype data. Individual pairs with PI_HAT ≥0.25 were identified and individuals with a low individual call rate

in the respective pairs were excluded from the analysis. In addition, clustering with multi-dimensional scaling (MDS) was performed based on the genotype data using PLINK software and the population enclosed by a red square was extracted (Figure S1). Besides these results, Japanese individuals were selected for analysis based on data from a questionnaire on birthplaces. In total, 1,041 individuals and 299,687 SNPs were selected for analysis through quality control. The reference human genome for SNP annotation was the hg19 (GRCh37) human genome assembly.

Genotype imputation

Genotype imputation was performed using Eagle[18] and Minimac 4[19] based on the Phase 3 reference panel in the 1000 Genomes Project[20]. After imputation, SNPs with a call rate <0.98, SNPs with a p value $<1\times10^{-3}$ in the Hardy-Weinberg equilibrium test, SNPs with Rsq, a precision measure for imputation results, <0.3, and SNPs with MAF <5% were excluded. A total of 5,447,137 SNPs were identified.

Phenotype data

Subjects were asked to fill out a questionnaire about wrinkles and sagging. The questionnaire asked subjects to select one image close to their current condition from six images of wrinkles at the outer corners of the eyes and nasolabial folds, and this was used as the phenotype (Figure S2 and Table S1). Furthermore, the questionnaire items included the presence or absence of UV protection on going out, smoking, and hormonal status (Table S1). Concerning UV protection, the subjects were instructed to select one of the following answers: “1. Always”, “2. Sometimes”, or “3. None”. Concerning smoking, they were instructed to select one of the following answers: “1.

Non-smoker", "2. Ex-smoker", "3. Smoker (1 to 10 cigarettes per day)", or "4. Smoker (≥11 cigarettes per day)". Concerning the hormonal status, they were instructed to select one of the following answers: "1. Before menopause" or "2. After menopause".

Statistical analysis

GWAS on each phenotype was performed by applying a multiple linear regression in an additive genetic model. To counteract departure from normality, a rank-based inverse normal transformation was applied to the aging level of wrinkles at the outer corners of the eyes. Age, UV protection, smoking, hormonal status and top 4 MDS coordinates were employed as covariates in all analyses. The thresholds for "suggestive" (1/n) and "significant" (0.05/n) were calculated using Genetic Type I Error Calculator (GEC) software[21]. The valid number of independent tests was estimated to be 1,125,999.74; therefore, the *p*-value thresholds used to identify significantly associated SNPs were 8.88×10^{-7} (suggestive) and 4.44×10^{-8} (significant). Since three data sets and two phenotypes were analyzed, the adjusted significance level was set at 7.40×10^{-9} ($4.44\times10^{-8}/6$). In addition, the false discovery rate (FDR) was adjusted by the Benjamini-Hochberg procedure (*q*-value). Manhattan plots and quantile-quantile plots were generated using the R package qqman[22]. Regional visualizations of GWAS results were prepared using the LocusZoom program[23].

eQTL analysis

We evaluated the expression quantitative trait loci (eQTL) signals of SNPs suggested to be associated with wrinkles and sagging using FUMA, a platform for the annotation and interpretation of GWAS results[24]. The following eQTL data sources were used for

the analyses, with details on tissue type and sample size available at https://fuma.ctglab.nl/tutorial#snp2gene: GTEx v6, Blood eQTL browser, BIOS QTL browser, BRAINEAC, GTEx v7, MuTHER, xQTLServer, CommonMind Consortium, eQTLGen, PsychENCODE, DICE, van der Wijst et al. scRNA eQTLs, GTEx v8, eQTL Catalogue, EyeGEx.

Cell culture and small interfering RNA (siRNA) transfection

Skin fibroblasts (SF8543), a cell line derived from a Japanese woman (RCB0608, RIKEN BioResource Center, Ibaraki, Japan), were cultured in DMEM (Nacalai Tesque, Kyoto, Japan) supplemented with 10% fetal bovine serum (Sigma–Aldrich, St. Louis, MO, USA). Cells were seeded on 12-well plates at a density of 1.5×10^4 cells per cm^2 and cultured for 24 h. Culture medium was replaced with OPTI-MEM® (Thermo Fisher Scientific, Waltham, MA, USA) containing Lipofectamine RNAiMAX (Thermo Fisher Scientific) and 100 nM of AccuTarget™ negative control siRNA (Bioneer, Daejeon, Korea) or AccuTarget™ Genome-wide Predesigned siRNA mixture targeting RAD21 (Bioneer) to avoid off-target effects. After a 4 h incubation, OPTI-MEM was replaced with fresh culture medium and cells were cultured for another 24 h.

RNA isolation and real-time RT-PCR

Total RNA was extracted from cultured SF8543 cells using RNAiso Plus (Takara Bio, Shiga, Japan), and cDNA was synthesized by PrimeScript™ RT Master Mix (Takara Bio). Real-time RT-PCR was performed with TB Green® Premix Ex Taq™ II (Takara Bio) using a StepOnePlus Real-Time PCR System (Thermo Fisher Scientific) in accordance with the manufacturer's protocol. The primers used for real-time RT-PCR

are listed in Table S2. Amplification was normalized to the *GAPDH* gene as an internal control and differences between samples were quantified based on the $\Delta\Delta$Ct method. Real-time RT-PCR analyses were performed in triplicate (n = 3). Statistical analyses were performed using the Student's *t*-test or Dunnett's test. Data are shown as the mean ± standard deviation. $p < 0.05$ was considered to be significant.

Measurement of cell growth

The proliferative potential of SF8543 cells was analyzed using the IncuCyte® ZOOM system (Essen BioScience, Ann Arbor, MI, USA). Cells were seeded on 96-well plates at a density of 1.5×10^4 cells per cm^2 and cultured for 24 h. Cells were transfected with siRNA, and medium was replaced 4 h later. After medium replacement, cells were photographed each day using the IncuCyte ZOOM system. Confluence at each time point was measured based on the images taken and compared. The cell growth analyses were performed in triplicate (n = 8). Statistical analyses were performed using the Student's *t*-test. Data are shown as the mean ± standard deviation. $p < 0.05$ was considered to be significant.

Results

GWAS on the contribution of genotypes to the development of wrinkles and sagging was conducted using three data sets: all subjects (n = 1,041), those younger than 59 years (n = 845), and those older than 60 years (n = 196). No SNPs met the level of significance in all subjects or in the group older than 60 years (data not shown). The GWAS results in the group younger than 59 years are shown in Figures 1 and S3. There was no genome inflation on analyses of wrinkles at the outer corners of the eyes or nasolabial folds. Five SNPs (rs2303098; $p = 3.39\times10^{-8}$, rs56391955; $p = 3.39\times10^{-8}$, rs67560822; $p = 3.50\times10^{-8}$, rs889126; $p = 3.78\times10^{-8}$, and rs57490083; $p = 3.99\times10^{-8}$) in the region of chromosome 19p13.2 were identified as SNPs associated with wrinkles at the outer corners of the eyes (Figure 1A and Table 1). The *p*-values of these SNPs did not exceed the adjusted significance level (7.40×10^{-9}), but the *q*-values were below 0.05; the possibility of false-positive findings may be low (Table S3). We then constructed a Locus Zoom plot and confirmed that these five SNPs were present in the *COL5A3* gene (Figure 2A). The SNPs rs56391955, rs67560822, rs889126 and rs57490083 were present in the intron of the *COL5A3* gene, while rs2303098 was found to be a missense SNP in the third exon that replaces arginine with histidine in the C-to-T base substitution in the reverse strand. We performed eQTL analysis in FUMA and found associations between these five SNPs and decreased or increased gene expression of *COL5A3* (Table S4). Type V collagen is one of the extracellular matrix (ECM) components in the dermis of skin and was previously shown to be important for elucidating the structure of collagen fibers and the composition of ECM[25]. It has also recently been reported to play a role in maintaining the function of dermal stem cells[26].

With respect to the nasolabial folds, there was no SNP exceeding the significance

level. Therefore, 5 high-order SNPs of which associations were suggested (rs111591235; $p = 8.02\times10^{-8}$, rs4876369; $p = 1.05\times10^{-7}$, rs6980503; $p = 1.25\times10^{-7}$, rs61027543; $p = 1.25\times10^{-7}$, and rs16889363; $p = 1.38\times10^{-7}$) are shown in Table 1. The *q*-values of these SNPs were below 0.05; the possibility of false-positive findings may be low (Table S3). One SNP, rs111591235, in the region of chromosome 5p15.2 was located in the intron of the *DNAH5* gene. Four SNPs in the region of chromosome 8q24.11 were present in the intron of the *SLC30A8* gene (Figures S4 and 2B). *DNAH5* is a gene encoding dynein protein, a motor protein, and is known to be expressed in the respiratory tract and testis[27]. *SLC30A8*, also known as *ZnT-8*, is a gene encoding a zinc transporter in intracellular vesicles and is predominantly expressed in the pancreas, but is considered to be poorly expressed in skin[28]. To identify candidate genes associated with rs111591235, rs4876369, rs6980503, rs61027543, and rs16889363, we performed eQTL analysis using FUMA (Table 2). No genes associated with rs111591235 were identified. In the 4 SNPs in 8q24.11, each risk allele negatively correlated with the expression of *RAD21* (rs4876369 ($p = 1.78\times10^{-10}$, risk allele; G, FDR 0), rs6980503 ($p = 1.47\times10^{-4}$, risk allele; A, FDR 0.305), rs61027543 ($p = 1.64\times10^{-4}$, risk allele; A, FDR 0.330), and rs16889363 ($p = 1.96\times10^{-4}$, risk allele; A, FDR 0.376)). RAD21 is a subunit of the cohesin complex and has been reported to affect sister chromatid adhesion, the recombination and repair of DNA, and transcription[29–32]. Previous studies confirmed that the suppression of *RAD21* expression by RNA interference induced cellular senescence, resulting in a decreased cellular proliferative potential[33–35]. However, limited information is currently available on the function of *RAD21* in skin. Therefore, we investigated whether *RAD21* was associated with aging and the cell proliferation of dermal fibroblasts using SF8543, a cell line derived from a Japanese female.

To elucidate the function of *RAD21* in dermal fibroblasts, we performed siRNA knockdown studies. *RAD21* mRNA expression levels were significantly lower in cells transfected with *RAD21* siRNA than in those transfected with a negative control (Figures 3A and S5). The expression of the senescence marker gene *CDKN1A* (*p21*) and the cell cycle-related genes *MKI67* and *CCNB1* was examined in *RAD21* knockdown cells. The expression level of *CDKN1A* (*p21*) significantly increased, while those of *MKI67* and *CCNB1* mRNA significantly decreased (Figure 3A). We then investigated the proliferative potential of cells in which *RAD21* was knocked down. Two days after transfection, cell proliferation was significantly lower in cells transfected with *RAD21* siRNA than in those transfected with the negative control (Figure 3B, C).

Finally, the effects of *RAD21* on ECM were investigated. The mRNA expression of *MMP1*, which degrades type I and III collagen (major components of ECM), and *MMP3*, which degrades type III collagen and proteoglycans, was significantly increased by the knockdown of *RAD21* (Figure 3A).

Discussion

In the field of beauty, wrinkles and sagging are the most prominent phenotypes of aging phenomena on the face, and various methods have been proposed for their prevention and improvement. Methods to protect against ultraviolet rays, which are primarily responsible for wrinkles and sagging, and those to promote the production of collagen, the main constituent of the dermis, have been extensively examined, and there is a growing demand for topical preparations containing ultraviolet-protective agents, exercises, and surgical treatment. Although the genetic predisposition of individuals to wrinkles and sagging has been reported in recent years, many issues remain unclear, which may be due in part to marked variations in the genetic predisposition of different ethnic groups to skin aging. In the present study, we conducted GWAS on wrinkles and sagging to clarify the genetic predisposition of Japanese women to aging phenomena on the face.

Regarding wrinkles at the outer corners of the eyes, five SNPs in the *COL5A3* gene were found to be significant (Figure 1A and Table 1). COL5A3 is an approximately 170 KDa protein consisting of 1745 amino acids and contains a signal peptide, non-collagenous domains, and collagenous domains. rs2303098 is located in the PARP domain, a subdomain of non-collagenous domain 3 (NC-3), which lies between the signal peptide of type V procollagen chain pro-α3 (V) and collagenous domain 2[36]. The PARP domain is conserved with pro-α1 (V), pro-α1 (XI), and pro-α2 (XI), and is also homologous to similar modules found in collagen types IX and XII[37,38]. The NC-3 domain of collagen types XII and XIV has been suggested to affect the interaction between collagen fibers and the migration of fibroblasts[38,39]. The SNPs identified in this study, including rs2303098, may influence the NC-3 domain function and *COL5A3*

expression. Actually, eQTL analysis showed that there were associations between these 5 SNPs and *COL5A3* gene expression in various organs, including blood (Table S4). The data on the skin could not be obtained, but these SNPs may also be associated with *COL5A3* gene expression in the skin; further analysis is needed. In the future, it must be further analyzed whether amino acid substitution influences the physical properties of collagen fibers and physiological function of fibroblasts when rs2303098 is a risk allele.

Regarding nasolabial folds, two genetic loci (5p15.2; *DNAH5,* 8q24.11; *SLC30A8*) were suggested to be associated (Figure 1B and Table 1). Since *DNAH5* is expressed in the respiratory tract and testis, and *SLC30A8* is predominantly expressed in the pancreas with rarely expressed in other tissues, we searched for genes that may be affected by the SNPs identified. Our eQTL analysis identified *RAD21* as a candidate gene whose expression may be affected by rs4876369, rs6980503, rs61027543, and rs16889363 (Table 2). RAD21 is a central component of the cohesin complex and has been reported to play a role in sister chromatid adhesion during mitosis, the recombination and repair of DNA, and transcription[29–32]. In cervical and breast cancer cells, the silencing of *RAD21* was previously show to increase tumor suppressors, such as p21, and, thus, induce cellular senescence, thereby decreasing the proliferative potential of cells[33–35]. In terms of proliferation, the down-regulation of proliferation markers, such as cyclin, has been reported. In the present study, the suppression of *RAD21* expression in dermal fibroblasts significantly increased the expression of senescence markers and significantly decreased the expression of the cell cycle-related genes *MKI67* and *CCNB1* (Figure 3A). This result suggests that *RAD21* is also involved in cellular senescence in dermal fibroblasts and may affect cell proliferation. Furthermore, the knockdown of *RAD21* significantly increased the expression levels of the ECM-

degrading enzymes *MMP1* and *MMP3* (Figure 3A). These results indicate that the SNPs identified in the present study affect the expression of *RAD21*, which decreases the proliferative capacity of fibroblasts in the dermis and promotes the degradation of ECM, thereby resulting in the development of wrinkles and sagging.

In this study, analysis was conducted in 3 populations: all female subjects, those younger than 59 years, and those older than 60 years. In those younger than 59 years, SNPs suggested to be associated with wrinkles and sagging were identified. The results of the association analysis of these SNPs in the all subjects and in those older than 60 years are shown in Table S5. In all subjects, the effect sizes and *p*-values were similar. On the other hand, there was no association in those older than 60 years. The number of samples from those older than 60 years was small, and this may have contributed to the above finding. In the future, a larger number of samples must be analyzed.

The use of UV protection is confounded with pigmentation levels, and is considered to have a genetic basis. Therefore, the use of UV protection in a covariate may be a collider bias. Since it is unclear whether the case is similar for wrinkles and sagging in the Japanese female population, we confirmed by excluding UV protection from the covariates. As a result, the effect sizes and *p*-values were similar to those when UV protection was included in the covariates (Table S6). Therefore, the SNPs identified in this study may not be false-positive findings related to the collider bias.

The SNPs associated with wrinkles and sagging in this study have not been reported in European or Chinese populations. They were first identified in the Japanese female population. Using a dataset from this study, we confirmed SNPs associated with wrinkles at the outer corners of the eyes (crow's feet, rs28392847) and nasolabial folds (rs76053540), which were identified by Liu et al.[10] However, there was no association

with each phenotype (Table S7). This suggests that Japanese and Chinese populations may have different ethnical backgrounds for wrinkles and sagging. In the future, the reproducibility of the SNPs identified in this study should be confirmed in various populations, and whether they are specific to a Japanese population or they have properties similar to a specific population must be confirmed.

In conclusion, we herein conducted GWAS on wrinkles and sagging in Japanese women and identified a genetic region (19p13.2; rs2303098, rs56391955, rs67560822, rs889126, rs57490083) associated with wrinkles at the outer corners of the eyes and two genetic regions (5p15.2; rs111591235, 8q24.11; rs4876369, rs6980503, rs61027543, rs16889363) for nasolabial folds. The SNPs identified in this study are hopeful, but they did not exceed the adjusted significance level (7.40×10^{-9}). In the future, the number of samples should be increased, and useful covariates, such as the body mass index (BMI), must be used. In addition, the reproducibility of these SNPs should be confirmed in another population. These are the limitations of this study. All of the SNPs and genetic regions identified in the present study may be associated with wrinkles and sagging, and may be used as markers to investigate the genetic predisposition of individuals to wrinkles and sagging.

Acknowledgments

We are indebted to all the volunteers who participated in the present study. We thank Eriko Morichi, Natsumi Nakao, Hiroaki Adachi, Yuichiro Ogata, Katsuma Miyachi, Masahiro Fujimura, Yoshie Ishii, Ayumi Sanada, and Ryoko Kawakami (Nippon Menard Cosmetic Co., Ltd., Aichi, Japan) for their assistance with volunteer recruitment and sample processing. We wish to acknowledge Division for Medical Research Engineering, Nagoya University Graduate School of Medicine, for usage of live-cell imaging system.

Conflicts of interest

The authors have a patent pending for the use of identified SNPs as markers to investigate the genetic predisposition. Therefore, GWAS data are not publicly available. The authors declare no other conflict of interest.

Author contributions

RO, YI, YH, and SH designed the research study. RO, YI, YH, TI, MKH, and TY performed the research and data analysis. RO wrote the manuscript. All authors critically revised the manuscript and approved the final draft.

References

1. El-Domyati M, Attia S, Saleh F, et al. Intrinsic aging vs. photoaging: A comparative histopathological, immunohistochemical, and ultrastructural study of skin. *Exp Dermatol*. 2002;11(5):398-405. doi:10.1034/j.1600-0625.2002.110502.x
2. Shuster S, Black MM, McVitie E. The influence of age and sex on skin thickness, skin collagen and density. *Br J Dermatol*. 1975;93(6):639-643. doi:10.1111/j.1365-2133.1975.tb05113.x
3. Talwar HS, Griffiths CE, Fisher GJ, Hamilton TA, Voorhees JJ. Reduced type I and type III procollagens in photodamaged adult human skin. *J Invest Dermatol*. 1995;105(2):285-290. doi:10.1111/1523-1747.ep12318471
4. Varani J, Dame MK, Rittie L, et al. Decreased collagen production in chronologically aged skin: roles of age-dependent alteration in fibroblast function and defective mechanical stimulation. *Am J Pathol*. 2006;168(6):1861-1868. doi:10.2353/ajpath.2006.051302
5. Fisher GJ, Datta SC, Talwar HS, et al. Molecular basis of sun-induced premature skin ageing and retinoid antagonism. *Nature*. 1996;379(6563):335-339. doi:10.1038/379335a0
6. Fisher GJ, Wang Z, Datta SC, Varani J, Kang S, Voorhees JJ. Pathophysiology of Premature Skin Aging Induced by Ultraviolet Light. *N Engl J Med*. 1997;337(20):1419-1429. doi:10.1056/nejm199711133372003
7. Sottile J, Mann DM, Diemer V, Millis AJ. Regulation of collagenase and collagenase mRNA production in early- and late-passage human diploid fibroblasts. *J Cell Physiol*. 1989;138(2):281-290. doi:10.1002/jcp.1041380209

8. Le Clerc S, Taing L, Ezzedine K, et al. A genome-wide association study in caucasian women points out a putative role of the STXBP5L gene in facial photoaging. *J Invest Dermatol*. 2013;133(4):929-935. doi:10.1038/jid.2012.458

9. Hamer MA, Pardo LM, Jacobs LC, et al. Facial Wrinkles in Europeans: A Genome-Wide Association Study. *J Invest Dermatol*. 2018;138(8):1877-1880. doi:10.1016/j.jid.2017.12.037

10. Liu Y, Gao W, Koellmann C, et al. Genome-wide scan identified genetic variants associated with skin aging in a Chinese female population. *J Dermatol Sci*. 2019;96(1):42-49. doi:10.1016/j.jdermsci.2019.08.010

11. Laville V, Le Clerc S, Ezzedine K, et al. A genome wide association study identifies new genes potentially associated with eyelid sagging. *Exp Dermatol*. 2019;28(8):892-898. doi:10.1111/exd.13559

12. Adhikari K, Mendoza-Revilla J, Sohail A, et al. A GWAS in Latin Americans highlights the convergent evolution of lighter skin pigmentation in Eurasia. *Nat Commun*. 2019;10(1):358. doi:10.1038/s41467-018-08147-0

13. Shido K, Kojima K, Yamasaki K, et al. Susceptibility Loci for Tanning Ability in the Japanese Population Identified by a Genome-Wide Association Study from the Tohoku Medical Megabank Project Cohort Study. *J Invest Dermatol*. 2019;139(7):1605-1608.e13. doi:10.1016/j.jid.2019.01.015

14. Zhang M, Li B, Wu S, et al. A Genome-Wide Association Study of Basal Transepidermal Water Loss Finds that Variants at 9q34.3 Are Associated with Skin Barrier Function. *J Invest Dermatol*. 2017;137(4):979-982. doi:10.1016/j.jid.2016.11.030

15. Inoue Y, Hasebe Y, Igarashi T, et al. Search for genetic loci involved in the

constitution and skin type of a Japanese women using a genome-wide association study. *Exp Dermatol*. Published online July 15, 2021. doi:10.1111/exd.14430

16. Baroni E do RV, Biondo-Simões M de LP, Auersvald A, et al. Influence of aging on the quality of the skin of white women: the role of collagen. *Acta Cir Bras*. 2012;27(10):736-740. doi:10.1590/s0102-86502012001000012

17. Chang CC, Chow CC, Tellier LC, Vattikuti S, Purcell SM, Lee JJ. Second-generation PLINK: rising to the challenge of larger and richer datasets. *Gigascience*. 2015;4:7. doi:10.1186/s13742-015-0047-8

18. Loh P-R, Danecek P, Palamara PF, et al. Reference-based phasing using the Haplotype Reference Consortium panel. *Nat Genet*. 2016;48(11):1443-1448. doi:10.1038/ng.3679

19. Das S, Forer L, Schönherr S, et al. Next-generation genotype imputation service and methods. *Nat Genet*. 2016;48(10):1284-1287. doi:10.1038/ng.3656

20. 1000 Genomes Project Consortium, Auton A, Brooks LD, et al. A global reference for human genetic variation. *Nature*. 2015;526(7571):68-74. doi:10.1038/nature15393

21. Li M-X, Yeung JMY, Cherny SS, Sham PC. Evaluating the effective numbers of independent tests and significant p-value thresholds in commercial genotyping arrays and public imputation reference datasets. *Hum Genet*. 2012;131(5):747-756. doi:10.1007/s00439-011-1118-2

22. D. Turner S. qqman: an R package for visualizing GWAS results using Q-Q and manhattan plots. *Prepr bioRxiv*. Published online 2014. doi:http://dx.doi.org/10.1101/005165

23. Pruim RJ, Welch RP, Sanna S, et al. LocusZoom: Regional visualization of

genome-wide association scan results. In: *Bioinformatics*. Vol 27. ; 2011:2336-2337. doi:10.1093/bioinformatics/btq419

24. Watanabe K, Taskesen E, van Bochoven A, Posthuma D. Functional mapping and annotation of genetic associations with FUMA. *Nat Commun*. 2017;8(1):1826. doi:10.1038/s41467-017-01261-5

25. Wenstrup RJ, Florer JB, Brunskill EW, Bell SM, Chervoneva I, Birk DE. Type V collagen controls the initiation of collagen fibril assembly. *J Biol Chem*. 2004;279(51):53331-53337. doi:10.1074/jbc.M409622200

26. Hasebe Y, Hasegawa S, Date Y, et al. Localization of collagen type 5 in the papillary dermis and its role in maintaining stem cell functions. *J Dermatol Sci*. 2018;89(2):205-207. doi:10.1016/j.jdermsci.2017.10.005

27. Hornef N, Olbrich H, Horvath J, et al. DNAH5 mutations are a common cause of primary ciliary dyskinesia with outer dynein arm defects. *Am J Respir Crit Care Med*. 2006;174(2):120-126. doi:10.1164/rccm.200601-084OC

28. Chimienti F, Devergnas S, Favier A, Seve M. Identification and cloning of a β-cell-specific zinc transporter, ZnT-8, localized into insulin secretory granules. *Diabetes*. 2004;53(9):2330-2337. doi:10.2337/diabetes.53.9.2330

29. Nasmyth K, Haering CH. Cohesin: its roles and mechanisms. *Annu Rev Genet*. 2009;43:525-558. doi:10.1146/annurev-genet-102108-134233

30. Hoque MT, Ishikawa F. Cohesin defects lead to premature sister chromatid separation, kinetochore dysfunction, and spindle-assembly checkpoint activation. *J Biol Chem*. 2002;277(44):42306-42314. doi:10.1074/jbc.M206836200

31. Watrin E, Peters J-M. Cohesin and DNA damage repair. *Exp Cell Res*. 2006;312(14):2687-2693. doi:10.1016/j.yexcr.2006.06.024

32. Wendt KS, Yoshida K, Itoh T, et al. Cohesin mediates transcriptional insulation by CCCTC-binding factor. *Nature*. 2008;451(7180):796-801. doi:10.1038/nature06634

33. Zhu S, Zhao L, Li Y, et al. Suppression of RAD21 Induces Senescence of MDA-MB-231 Human Breast Cancer Cells Through RB1 Pathway Activation Via c-Myc Downregulation. *J Cell Biochem*. 2016;117(6):1359-1369. doi:10.1002/jcb.25426

34. Atienza JM, Roth RB, Rosette C, et al. Suppression of RAD21 gene expression decreases cell growth and enhances cytotoxicity of etoposide and bleomycin in human breast cancer cells. *Mol Cancer Ther*. 2005;4(3):361-368. doi:10.1158/1535-7163.MCT-04-0241

35. Xia L, Wang M, Li H, Tang X, Chen F, Cui J. The effect of aberrant expression and genetic polymorphisms of Rad21 on cervical cancer biology. *Cancer Med*. 2018;7(7):3393-3405. doi:10.1002/cam4.1592

36. Imamura Y, Scott IC, Greenspan DS. The pro-alpha3(V) collagen chain. Complete primary structure, expression domains in adult and developing tissues, and comparison to the structures and expression domains of the other types V and XI procollagen chains. *J Biol Chem*. 2000;275(12):8749-8759. doi:10.1074/jbc.275.12.8749

37. Bork P. The modular architecture of vertebrate collagens. *FEBS Lett*. 1992;307(1):49-54. doi:10.1016/0014-5793(92)80900-2

38. Akutsu N, Milbury CM, Burgeson RE, Nishiyama T. Effect of type XII or XIV collagen NC-3 domain on the human dermal fibroblast migration into reconstituted collagen gel. *Exp Dermatol*. 1999;8(1):17-21. doi:10.1111/j.1600-

0625.1999.tb00343.x

39. Nishiyama T, McDonough AM, Bruns RR, Burgeson RE. Type XII and XIV collagens mediate interactions between banded collagen fibers in vitro and may modulate extracellular matrix deformability. *J Biol Chem*. 1994;269(45):28193-28199. doi:10.1016/s0021-9258(18)46913-x

Figure legends

Figure 1. Manhattan plots of GWAS with aging phenotypes in Japanese females.
Manhattan plots of GWAS with wrinkles (A) and nasolabial folds (B). The red horizontal line indicates a significance threshold of $p = 4.44\times10^{-8}$ and the blue line indicates a suggestive significance threshold of $p = 8.88\times10^{-7}$. Genetic regions that reached significance or suggestive significance are indicated by arrows.

Figure 2. Regional association plots for rs2303098 and rs4876369.
(A and B) Association results of both genotyped and imputed SNPs are plotted as the distribution of -log10 (*p*-values) along the physical position on each chromosome. Top SNPs are shown in purple, while other SNPs are colored based on the degree of their linkage disequilibrium with the top SNPs, according to the r^2 legend (top left or right). The light blue line shows the recombination rate expressed in centiMorgan (cM) by Megabase (Mb). Genes in the region are indicated at the bottom. Exons are shown by filled boxes, and the arrows on genes reflect the transcription direction.

Figure 3. *RAD21* knockdown effects in fibroblasts.
(A-C) siRNA for a negative control (siNC) or siRNA targeting *RAD21* (siRAD21) was transfected into SF8543 cells. (A) Gene expression levels were examined by real-time RT-PCR. Values are expressed as the mean ± SD. *p*-values were examined by the Student's *t*-test (n = 3, $*p < 0.05$, $**p < 0.01$, $***p < 0.001$, vs. siNC). (B) Typical images of cells 6 days after siRNA transfection. Scale bar = 250 μm. (C) Cell growth was assessed by measuring cell confluence with the IncuCyte ZOOM system. Values are expressed as the mean ± SD. *p*-values were examined by the Student's *t*-test (n = 8,

$^{**}p < 0.01$, $^{***}p < 0.001$, vs. siNC)

Figure S1 Multidimensional scaling (MDS) in this GWAS.

MDS shows the population structure of individuals. The area boxed by the red square indicates the Japanese population.

Figure S2 Visual scale used to assess wrinkles and nasolabial folds.

Subjects were asked to select their current wrinkles and nasolabial folds from the visual scale.

Figure S3 Quantile-quantile plot of the association study.

(A and B) Comparison between observed and expected under the null hypothesis distributions of $-\log_{10}$ (*p*-values).

Figure S4 Regional association plot for rs111591235.

Association results of both genotyped and imputed SNPs are plotted as the distribution of -log10 (*p*-values) along the physical position on the chromosome. Top SNP is shown in purple, while other SNPs are colored based on the degree of their linkage disequilibrium with the top SNP, according to the r^2 legend (top right). The light blue line shows the recombination rate expressed in centiMorgan (cM) by Megabase (Mb). A gene in the region is indicated at the bottom. Exons are shown by filled boxes, and the arrows on genes reflect the transcription direction.

Figure S5. Verification of knockdown effects of *RAD21* by siRNA.

siRNA for a negative control (siNC) or siRNA targeting *RAD21* (#1-#3 or Mixture) was transfected into SF8543 cells and *RAD21* gene expression levels were examined by real-time RT-PCR. Values are shown as the mean ± SD. *p*-values were examined by Dunnett's test (n = 3, ***$p < 0.001$, vs. siNC).

Table 1

Association results for significant and suggestive SNPs in this study.

SNP	Locus	Position	Ref	Alt	EA	Phenotype	Gene	Function	EAF	β	SE	*p*-value	Imputed or Direct Typing
rs2303098	19p13.2	10116508	C	T	T	Wrinkles	*COL5A3*	Missense	0.10	0.322	0.058	3.39×10^{-8}	Imputed
rs56391955	19p13.2	10117304	C	T	T	Wrinkles	*COL5A3*	Intron	0.10	0.322	0.058	3.39×10^{-8}	Imputed
rs67560822	19p13.2	10115580	C	T	T	Wrinkles	*COL5A3*	Intron	0.10	0.321	0.058	3.50×10^{-8}	Imputed
rs889126	19p13.2	10115424	G	A	A	Wrinkles	*COL5A3*	Intron	0.11	0.315	0.057	3.78×10^{-8}	Direct
rs57490083	19p13.2	10113280	C	T	T	Wrinkles	*COL5A3*	Intron	0.18	0.255	0.046	3.99×10^{-8}	Imputed
rs111591235	5p15.2	13713218	A	G	G	Nasolabial folds	*DNAH5*	Intron	0.18	0.273	0.050	8.02×10^{-8}	Imputed
rs4876369	8q24.11	118163504	A	G	G	Nasolabial folds	*SLC30A8*	Intron	0.10	0.382	0.071	1.05×10^{-7}	Imputed
rs6980503	8q24.11	118078751	G	A	A	Nasolabial folds	*SLC30A8*	Intron	0.11	0.349	0.065	1.25×10^{-7}	Direct
rs61027543	8q24.11	118081568	G	A	A	Nasolabial folds	*SLC30A8*	Intron	0.11	0.349	0.065	1.25×10^{-7}	Imputed
rs16889363	8q24.11	118061952	G	A	A	Nasolabial folds	*SLC30A8*	Intron	0.11	0.352	0.066	1.38×10^{-7}	Imputed

Ref, reference allele, Alt, alternative allele; EA, effect allele; EAF, effect allele frequency; β, beta coefficient; SE, standard error.

Table 2

eQTL analysis of nasolabial folds related SNPs.

SNP	Database	Tissue	Tested	Risk	Gene	Direction	*p*-value	FDR
rs4876369	eQTLGen	Blood	G	G	*RAD21*	-	1.78×10^{-10}	0
rs4876369	eQTLGen	Blood	G	G	*UTP23*	+	1.48×10^{-5}	0.041
rs4876369	PsychENCODE	Brain	G	G	*AARD*	-	5.13×10^{-4}	0.034
rs4876369	GTEx/v8	Adipose_Visceral_Omentum	G	G	*EXT1*	+	3.15×10^{-4}	NA
rs4876369	GTEx/v8	Brain_Caudate_basal_ganglia	G	G	*UTP23*	+	3.80×10^{-4}	NA
rs4876369	GTEx/v8	Uterus	G	G	*AARD*	-	4.97×10^{-4}	NA
rs4876369	GTEx/v7	Prostate	G	G	*EIF3H*	-	8.50×10^{-4}	NA
rs4876369	GTEx/v7	Uterus	G	G	*AARD*	-	2.99×10^{-5}	NA
rs4876369	GTEx/v6	Testis	G	G	*SLC30A8*	+	2.89×10^{-4}	NA
rs4876369	GTEx/v6	Uterus	G	G	*AARD*	-	4.38×10^{-4}	NA
rs6980503	eQTLGen	Blood	A	A	*RAD21*	-	1.47×10^{-4}	0.305
rs6980503	GTEx/v8	Brain_Caudate_basal_ganglia	A	A	*UTP23*	+	3.14×10^{-5}	0.037
rs6980503	GTEx/v7	Prostate	A	A	*EIF3H*	-	9.98×10^{-4}	NA
rs61027543	eQTLGen	Blood	A	A	*RAD21*	-	1.64×10^{-4}	0.330
rs61027543	GTEx/v8	Brain_Caudate_basal_ganglia	A	A	*UTP23*	+	3.14×10^{-5}	0.037
rs61027543	GTEx/v7	Prostate	A	A	*EIF3H*	-	9.98×10^{-4}	NA
rs16889363	eQTLGen	Blood	A	A	*RAD21*	-	1.96×10^{-4}	0.376
rs16889363	GTEx/v8	Brain_Caudate_basal_ganglia	A	A	*UTP23*	+	1.13×10^{-4}	NA
rs16889363	GTEx/v7	Prostate	A	A	*EIF3H*	-	8.73×10^{-4}	NA

Tested, tested allele; Risk, risk increasing allele, Direction, aligned direction; FDR, false discovery rate; +, risk increasing allele increases the expression of the gene; -, risk increasing allele decreases the expression of the gene; NA, not available.

Fig. 1

(A)

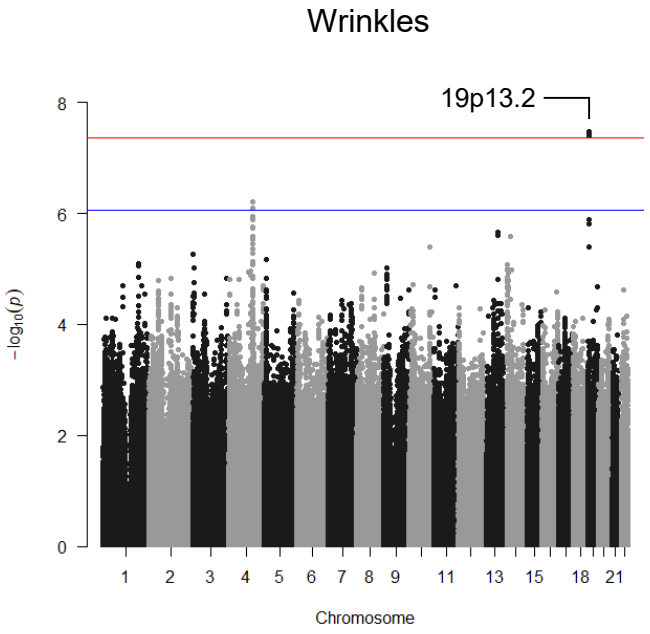
Wrinkles
19p13.2
8
6
4
2
0
−log10(p)
1
2
3
4
5
6
7
8
9
11
13
15
18
21
Chromosome

(B)

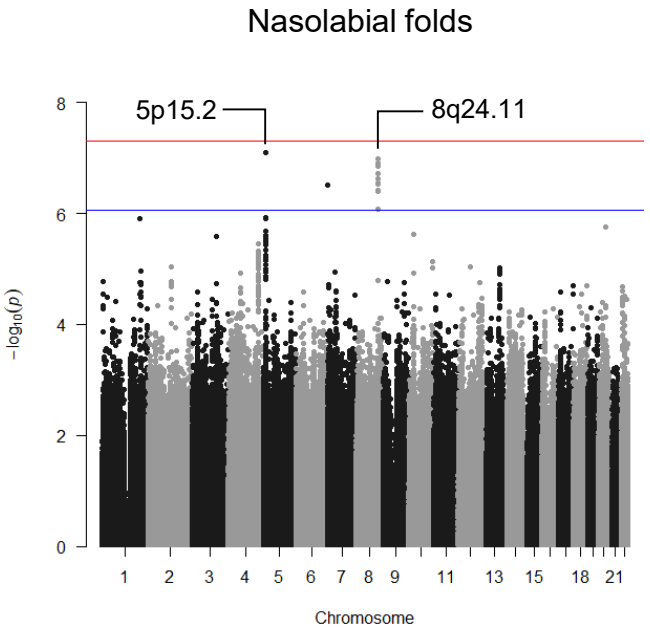
Nasolabial folds
5p15.2
8q24.11
8
6
4
2
0
−log10(p)
1
2
3
4
5
6
7
8
9
11
13
15
18
21
Chromosome

Fig. 2

(A)

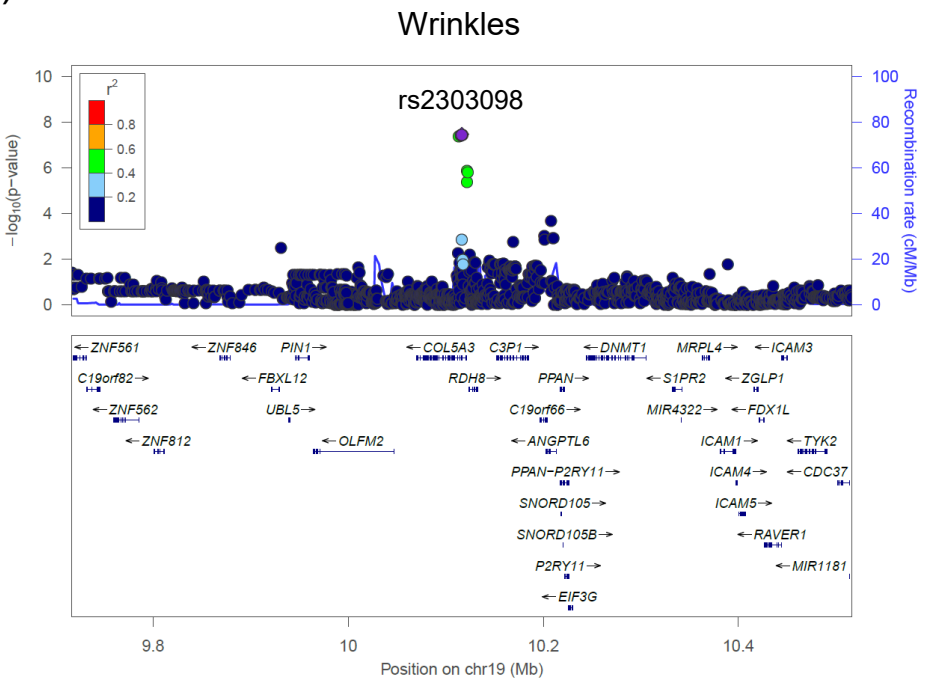
Wrinkles
rs2303098
r²
0.8
0.6
0.4
0.2
−log10(p−value)
Recombination rate (cM/Mb)
ZNF561
ZNF846
PIN1
COL5A3
C3P1
DNMT1
MRPL4
ICAM3
C19orf82
FBXL12
RDH8
PPAN
S1PR2
ZGLP1
ZNF562
UBL5
C19orf66
MIR4322
FDX1L
ZNF812
OLFM2
ANGPTL6
ICAM1
TYK2
PPAN−P2RY11
ICAM4
CDC37
SNORD105
ICAM5
SNORD105B
RAVER1
P2RY11
MIR1181
EIF3G
9.8
10
10.2
10.4
Position on chr19 (Mb)

(B)

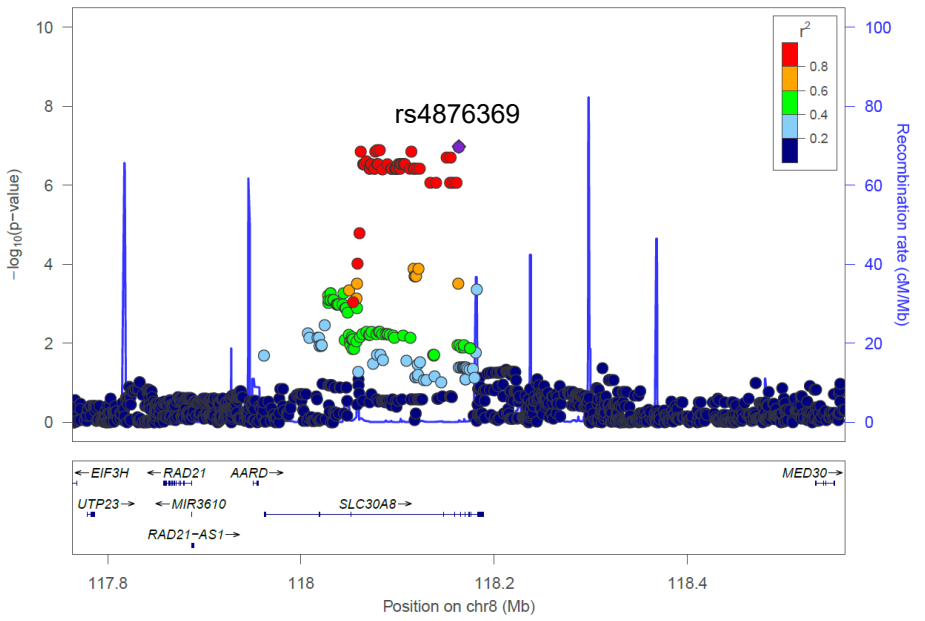
Nasolabial folds
rs4876369
r²
0.8
0.6
0.4
0.2
−log10(p−value)
Recombination rate (cM/Mb)
EIF3H
RAD21
AARD
MED30
UTP23
MIR3610
SLC30A8
RAD21−AS1
117.8
118
118.2
118.4
Position on chr8 (Mb)

Fig. 3

(A)

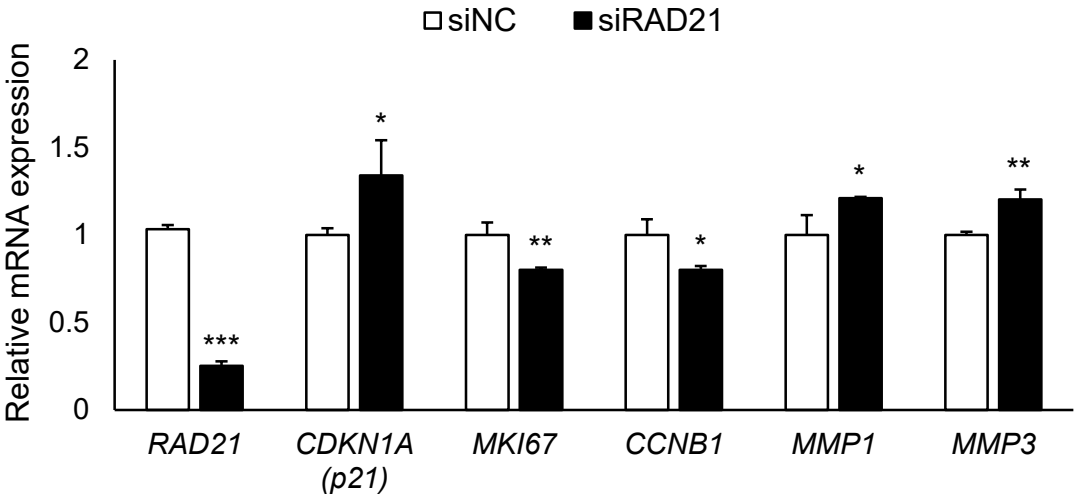
siNC
siRAD21
Relative mRNA expression
2
1.5
1
0.5
0
***
*
**
*
*
**
RAD21
CDKN1A (p21)
MKI67
CCNB1
MMP1
MMP3

(B)

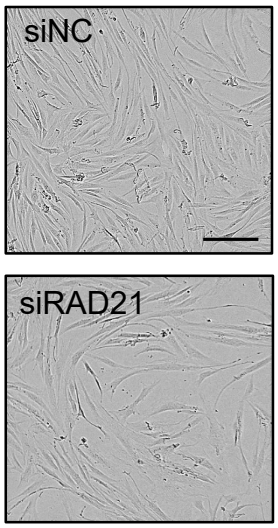
siNC
siRAD21

(C)

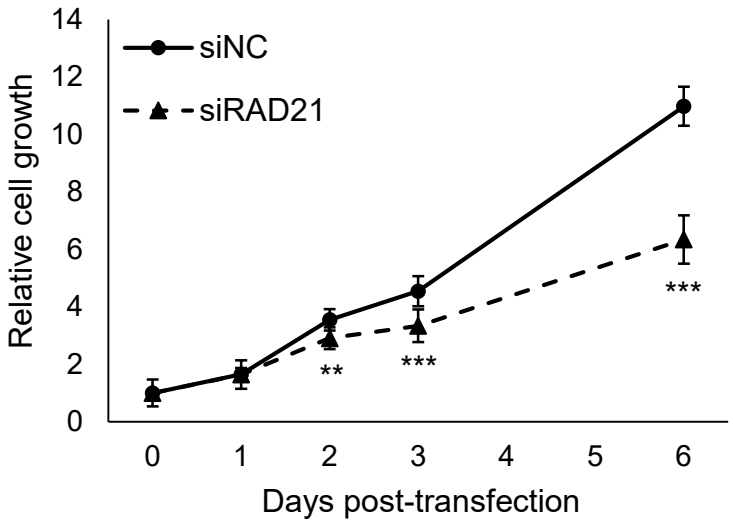
siNC
siRAD21
Relative cell growth
14
12
10
8
6
4
2
0
**
***
***
0
1
2
3
4
5
6
Days post-transfection

Figure S1

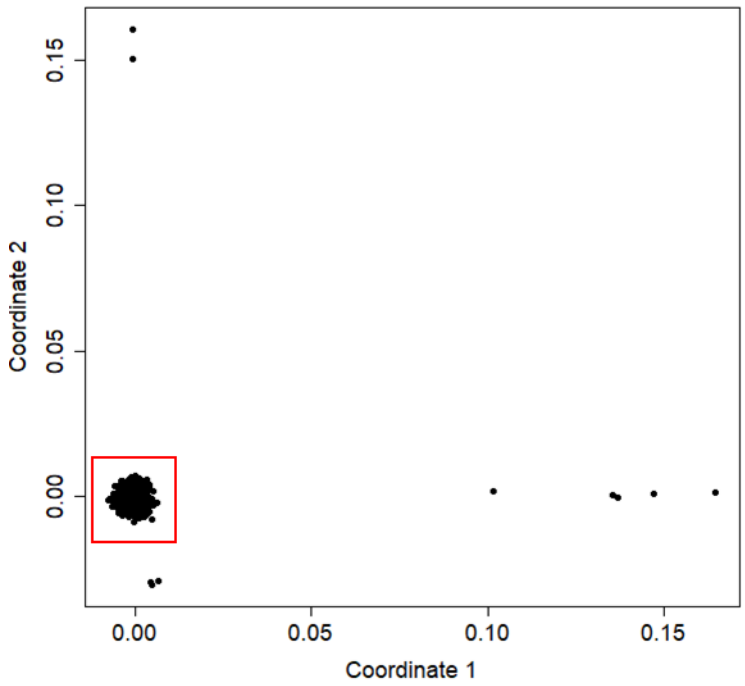

Figure S2

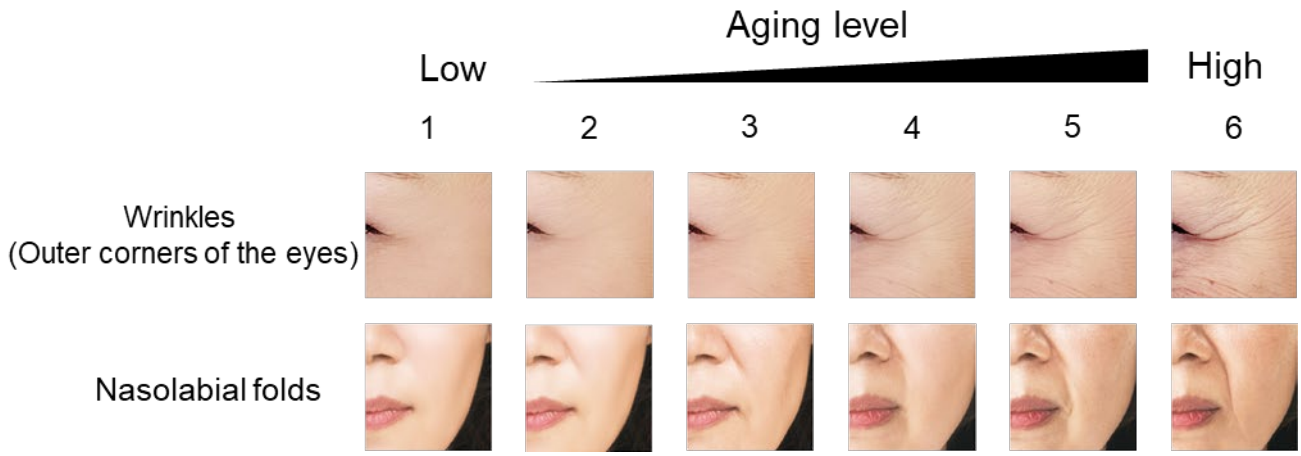
Aging level
Low
High
1
2
3
4
5
6
Wrinkles
(Outer corners of the eyes)
Nasolabial folds

Figure S3

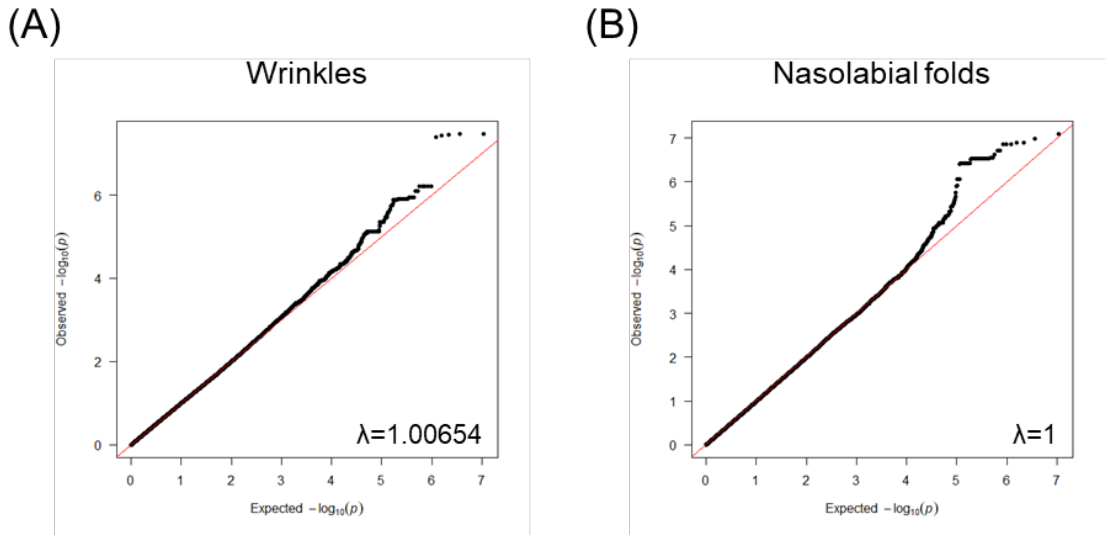
(A)
Wrinkles
λ=1.00654
Observed $-\log_{10}(p)$
Expected $-\log_{10}(p)$
(B)
Nasolabial folds
λ=1
Observed $-\log_{10}(p)$
Expected $-\log_{10}(p)$

Figure S4

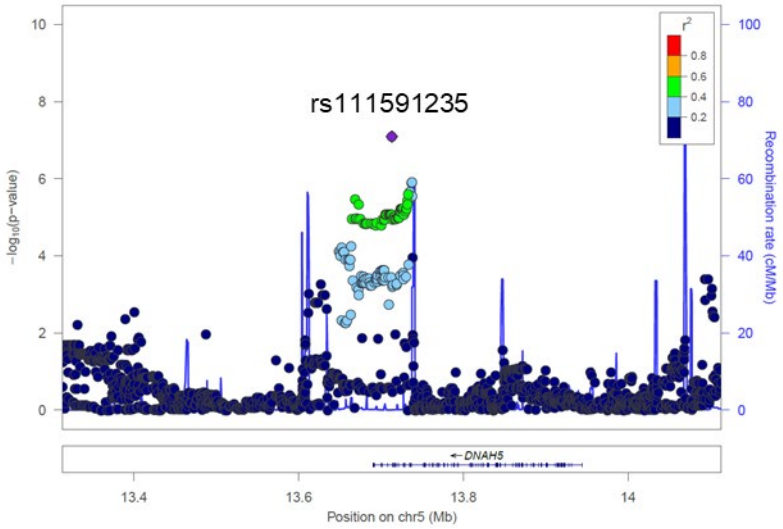
rs111591235
r²
0.8
0.6
0.4
0.2
10
8
6
4
2
0
100
80
60
40
20
0
Recombination rate (cM/Mb)
−log10(p−value)
DNAH5
13.4
13.6
13.8
14
Position on chr5 (Mb)

Figure S5

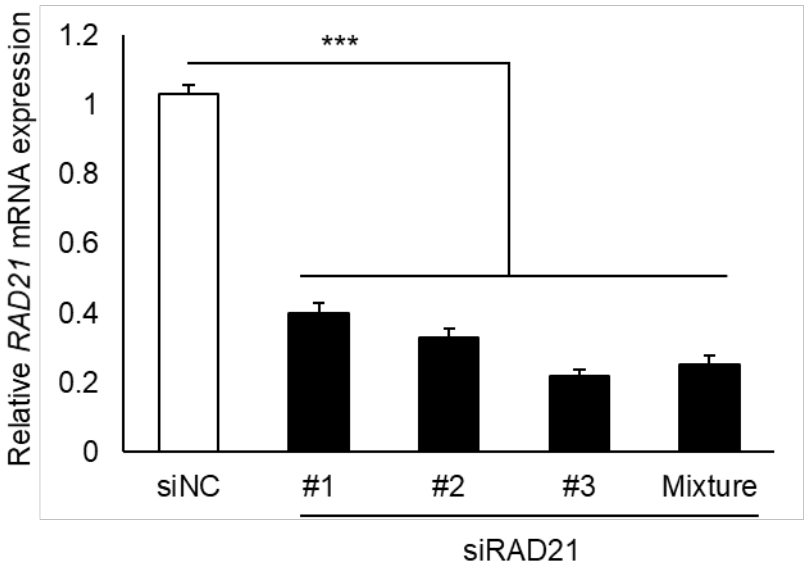
Relative RAD21 mRNA expression
1.2
1
0.8
0.6
0.4
0.2
0
***
siNC
#1
#2
#3
Mixture
siRAD21

Table S1

Description of the study population

Sample size		All female (n=1041)	Female under 59 (n=845)	Female older than 60 (n=196)
Age(years)	Mean(SD)	49.0(12.1)	44.8(8.7)	67.3(6.1)
	Min-Max	21-95	21-59	60-95
Aging level				
Wrinkles(outer corners of the eyes)				
1	%Yes(n)	34.1(355)	40.6(343)	6.1(12)
2	%Yes(n)	33.1(345)	35.4(299)	23.5(46)
3	%Yes(n)	20.8(217)	17.9(151)	33.7(66)
4	%Yes(n)	9.6(100)	5.2(44)	28.6(56)
5	%Yes(n)	1.9(20)	0.7(6)	7.1(14)
6	%Yes(n)	0.4(4)	0.2(2)	1.0(2)
Nasolabial folds				
1	%Yes(n)	11.3(118)	14.0(118)	0(0)
2	%Yes(n)	39.9(415)	46.6(394)	10.7(21)
3	%Yes(n)	22.2(231)	22.8(193)	19.4(38)
4	%Yes(n)	18.6(194)	13.7(116)	39.8(78)
5	%Yes(n)	5.8(60)	2.0(17)	21.9(43)
6	%Yes(n)	2.0(21)	0.7(6)	7.7(15)
unanswered	%Yes(n)	0.2(2)	0.1(1)	0.5(1)
UV protection				
Always	%Yes(n)	80.1(833)	79.6(673)	82.1(160)
Sometimes	%Yes(n)	17.4(181)	17.8(150)	15.9(31)
None	%Yes(n)	2.5(26)	2.6(22)	2.1(4)
Smoking				
Non-smokers	%Yes(n)	68.9(717)	67.6(571)	74.5(146)
Ex-smokers	%Yes(n)	19.2(200)	19.9(168)	16.3(32)
Smokers(1-10 cigarettes per day)	%Yes(n)	6.0(62)	6.3(53)	4.6(9)
Smokers(≥11 cigarettes per day)	%Yes(n)	6.0(62)	6.3(53)	4.6(9)
Hormonal status				
Menopause	%Yes(n)	41.6(433)	28.3(239)	99.0(194)

Table S2

Primers used for real-time RT-PCR.

Gene	Foward sequence	Reverse sequence
RAD21	ATGGCATTACGGACATCAGG	CACATCGATGTCATCTAAGTCAGG
CDKN1A	CCTTCCAGCTCCTGTAACATACTG	AGAAACGGGAACCAGGACAC
MKI67	AGACGCCTGGTTACTATCAAAAG	GGAAGCTGGATACGGATGTCA
CCNB1	GGCCTCTACCTTTGCACTTCCT	GCTCGACATCAACCTCTCCAA
MMP1	GGGAGATCATCGGGACAACTC	TGAGCATCCCCTCCAATACC
MMP3	GATGATGAACAATGGACAAAGGATAC	CAATTTCATGAGCAGCAACGA
GAPDH	TGCACCACCAACTGCTTAGC	TCTTCTGGGTGGCAGTGATG

Table S3

The FDR-adjusted *p*-value (*q*-value).

SNP	Phenotype	FDR
rs2303098	Wrinkles	0.043
rs56391955	Wrinkles	0.043
rs67560822	Wrinkles	0.043
rs889126	Wrinkles	0.043
rs57490083	Wrinkles	0.043
rs111591235	Nasolabial folds	0.044
rs4876369	Nasolabial folds	0.044
rs6980503	Nasolabial folds	0.044
rs61027543	Nasolabial folds	0.044
rs16889363	Nasolabial folds	0.044

Table S4

eQTL analysis of wrinkles related SNPs.

SNP	Database	Tissue	Tested	Risk	Gene	Direction	*p*-value	FDR
rs2303098	eQTLcatalogue	Blood	C	T	*COL5A3*	-	2.48.E-04	1
rs2303098	eQTLcatalogue	Macrophage	C	T	*COL5A3*	+	3.23.E-04	1.000
rs2303098	eQTLcatalogue	Blood	C	T	*COL5A3*	-	1.91.E-04	1.000
rs2303098	eQTLGen	Blood	T	T	*COL5A3*	+	1.35.E-22	0.000
rs2303098	BIOSQTL	Blood	T	T	*COL5A3*	+	1.01.E-06	0.001
rs2303098	BIOSQTL	Blood	T	T	*COL5A3*	+	6.16.E-07	0.001
rs2303098	GTEx/v8	Whole_Blood	T	T	*COL5A3*	+	1.20.E-06	0.000
rs2303098	GTEx/v8	Liver	T	T	*COL5A3*	+	4.23.E-04	NA
rs2303098	GTEx/v8	Nerve_Tibial	T	T	*COL5A3*	+	1.05.E-09	0.000
rs2303098	GTEx/v7	Whole_Blood	T	T	*COL5A3*	+	9.54.E-04	NA
rs2303098	GTEx/v7	Nerve_Tibial	T	T	*COL5A3*	+	4.66.E-05	0.008
rs2303098	GTEx/v6	Whole_Blood	T	T	*COL5A3*	+	3.44.E-04	NA
rs2303098	GTEx/v6	Esophagus_Mucosa	T	T	*COL5A3*	+	7.22.E-04	NA
rs56391955	eQTLcatalogue	Blood	C	T	*COL5A3*	-	2.85.E-04	1.000
rs56391955	eQTLcatalogue	Macrophage	C	T	*COL5A3*	+	3.69.E-04	1.000
rs56391955	eQTLcatalogue	Blood	C	T	*COL5A3*	-	1.91.E-04	1.000
rs56391955	eQTLGen	Blood	T	T	*COL5A3*	+	6.23.E-22	0.000
rs56391955	BIOSQTL	Blood	T	T	*COL5A3*	+	1.39.E-06	0.001
rs56391955	BIOSQTL	Blood	T	T	*COL5A3*	+	7.82.E-07	0.001
rs56391955	GTEx/v8	Whole_Blood	T	T	*COL5A3*	+	1.20E-06	9.28E-64
rs56391955	GTEx/v8	Liver	T	T	*COL5A3*	+	0.000	NA
rs56391955	GTEx/v8	Nerve_Tibial	T	T	*COL5A3*	+	1.05E-09	4.34E-07
rs56391955	GTEx/v7	Whole_Blood	T	T	*COL5A3*	+	0.001	NA
rs56391955	GTEx/v7	Nerve_Tibial	T	T	*COL5A3*	+	4.69E-05	0.008
rs56391955	GTEx/v6	Whole_Blood	T	T	*COL5A3*	+	0.000	NA
rs56391955	GTEx/v6	Esophagus_Mucosa	T	T	*COL5A3*	+	0.001	NA
rs67560822	eQTLcatalogue	Blood	C	T	*COL5A3*	-	0.000	1
rs67560822	eQTLcatalogue	Macrophage	C	T	*COL5A3*	+	0.000	1
rs67560822	eQTLcatalogue	Blood	C	T	*COL5A3*	-	0.000	1
rs67560822	DICE	TFH CD4 T cells	T	T	*COL5A3*	+	5.54E-05	0.049
rs67560822	DICE	TH17 CD4 T cells	T	T	*COL5A3*	+	2.90E-05	0.049
rs67560822	eQTLGen	Blood	T	T	*COL5A3*	+	1.53E-22	0
rs67560822	BIOSQTL	Blood	T	T	*COL5A3*	+	1.20E-06	0.001
rs67560822	BIOSQTL	Blood	T	T	*COL5A3*	+	8.77E-07	0.001
rs67560822	GTEx/v8	Whole_Blood	T	T	*COL5A3*	+	1.37E-06	9.28E-64
rs67560822	GTEx/v8	Liver	T	T	*COL5A3*	+	0.001	NA
rs67560822	GTEx/v8	Nerve_Tibial	T	T	*COL5A3*	+	3.79E-09	4.34E-07
rs67560822	GTEx/v7	Nerve_Tibial	T	T	*COL5A3*	+	9.96E-05	NA

rs67560822	GTEx/v6	Whole_Blood	T	T	*COL5A3*	+	0.000	NA
rs67560822	GTEx/v6	Esophagus_Mucosa	T	T	*COL5A3*	+	0.001	NA
rs889126	eQTLcatalogue	Blood	G	A	*COL5A3*	-	4.65E-07	0.002
rs889126	eQTLcatalogue	Blood	G	A	*COL5A3*	-	3.01E-05	1
rs889126	DICE	TFH CD4 T cells	A	A	*COL5A3*	+	5.54E-05	0.049
rs889126	DICE	TH17 CD4 T cells	A	A	*COL5A3*	+	2.90E-05	0.049
rs889126	eQTLGen	Blood	A	A	*COL5A3*	+	1.61E-33	0
rs889126	BIOSQTL	Blood	A	A	*COL5A3*	+	6.19E-08	5.64E-05
rs889126	BIOSQTL	Blood	A	A	*COL5A3*	+	2.47E-09	6.06E-06
rs889126	GTEx/v8	Whole_Blood	A	A	*COL5A3*	+	1.79E-08	9.28E-64
rs889126	GTEx/v8	Liver	A	A	*COL5A3*	+	0.000	NA
rs889126	GTEx/v8	Nerve_Tibial	A	A	*COL5A3*	+	1.69E-05	4.34E-07
rs889126	GTEx/v7	Whole_Blood	A	A	*COL5A3*	+	0.001	NA
rs889126	GTEx/v6	Whole_Blood	A	A	*COL5A3*	+	1.96E-05	NA
rs57490083	eQTLcatalogue	Blood	C	T	*COL5A3*	-	1.08E-05	1
rs57490083	eQTLcatalogue	Blood	C	T	*COL5A3*	-	1.16E-05	1
rs57490083	eQTLGen	Blood	T	T	*COL5A3*	+	7.80E-29	0
rs57490083	BIOSQTL	Blood	T	T	*COL5A3*	+	5.03E-08	4.54E-05
rs57490083	BIOSQTL	Blood	T	T	*COL5A3*	+	2.33E-09	6.06E-06
rs57490083	GTEx/v8	Whole_Blood	T	T	*COL5A3*	+	2.84E-08	9.28E-64
rs57490083	GTEx/v8	Liver	T	T	*COL5A3*	+	4.85E-05	NA
rs57490083	GTEx/v8	Nerve_Tibial	T	T	*COL5A3*	+	0.000	4.34E-07
rs57490083	GTEx/v6	Whole_Blood	T	T	*COL5A3*	+	0.000	NA

Tested, tested allele; Risk, risk increasing allele, Direction, aligned direction; FDR, false discovery rate; +, risk increasing allele increases the expression of the gene; -, risk increasing allele decreases the expression of the gene; NA, not available.

Table S5

Association results of the lead SNPs in the all female and the older than 60 populations.

SNP	Phenotype	Population	β	SE	*p*-value
rs2303098	Wrinkles	All female	0.228	0.051	7.58×10^{-6}
		Female older than 60	-0.190	0.161	0.237
rs56391955	Wrinkles	All female	0.228	0.051	7.58×10^{-6}
		Female older than 60	-0.190	0.161	0.237
rs67560822	Wrinkles	All female	0.217	0.050	1.90×10^{-5}
		Female older than 60	-0.236	0.158	0.138
rs889126	Wrinkles	All female	0.224	0.050	7.87×10^{-6}
		Female older than 60	-0.190	0.161	0.237
rs57490083	Wrinkles	All female	0.169	0.040	2.55×10^{-5}
		Female older than 60	-0.126	0.119	0.294
rs111591235	Nasolabial folds	All female	0.231	0.048	1.96×10^{-6}
		Female older than 60	0.076	0.138	0.583
rs4876369	Nasolabial folds	All female	0.309	0.067	4.54×10^{-6}
		Female older than 60	0.066	0.180	0.712
rs6980503	Nasolabial folds	All female	0.284	0.061	3.70×10^{-6}
		Female older than 60	0.096	0.160	0.549
rs61027543	Nasolabial folds	All female	0.284	0.061	3.70×10^{-6}
		Female older than 60	0.096	0.160	0.549
rs16889363	Nasolabial folds	All female	0.292	0.062	2.88×10^{-6}
		Female older than 60	0.099	0.163	0.545

Table S6

Association results of the lead SNPs excluding UV protection from covariates in the female under 59 years population.

SNP	Phenotype	β	SE	*p*-value
rs2303098	Wrinkles	0.323	0.058	3.26×10^{-8}
rs56391955	Wrinkles	0.323	0.058	3.26×10^{-8}
rs67560822	Wrinkles	0.322	0.058	3.30×10^{-8}
rs889126	Wrinkles	0.318	0.057	3.23×10^{-8}
rs57490083	Wrinkles	0.259	0.046	2.60×10^{-8}
rs111591235	Nasolabial folds	0.271	0.051	1.07×10^{-7}
rs4876369	Nasolabial folds	0.375	0.071	1.96×10^{-7}
rs6980503	Nasolabial folds	0.345	0.066	2.02×10^{-7}
rs61027543	Nasolabial folds	0.345	0.066	2.02×10^{-7}
rs16889363	Nasolabial folds	0.347	0.067	2.27×10^{-7}

Table S7

Association results of the lead SNPs associated with wrinkles and sagging in Chinese female population.

SNP	Locus	Position	Phenotype	Gene	Function	Study	β	SE	*p*-value
rs28392847	15q21.1	49248001	Wrinkles(Crow's feet)	*SHC4*	Intron	All female	0.001	0.033	0.983
						Female under 59	0.012	0.039	0.765
						Female older than 60	-0.070	0.098	0.476
rs76053540	16p13.11	15927276	Nasolabial folds	*MYH11*	Intron	All female	-0.034	0.065	0.605
						Female under 59	-0.031	0.068	0.652
						Female older than 60	-0.034	0.161	0.834